UC Berkeley

UC Berkeley Previously Published Works

Title

Electrical breakdown in tissue electroporation

Permalink

https://escholarship.org/uc/item/6jw1f42m

Journal

Biochemical and Biophysical Research Communications, 467(4)

ISSN

0006-291X

Authors

Guenther, Enric
Klein, Nina
Mikus, Paul
et al.

Publication Date

2015-11-01

DOI

10.1016/j.bbrc.2015.10.072

Peer reviewed

eScholarship.org Powered by the California Digital Library
University of California

Accepted Manuscript

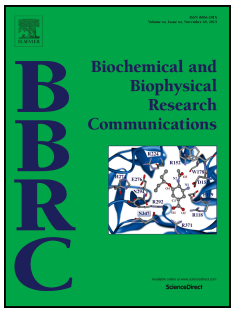

Electrical breakdown in tissue electroporation

Enric Guenther, Nina Klein, Paul Mikus, Michael K. Stehling, Boris Rubinsky

PII: S0006-291X(15)30771-3

DOI: 10.1016/j.bbrc.2015.10.072

Reference: YBBRC 34756

To appear in: *Biochemical and Biophysical Research Communications*

Received Date: 1 October 2015

Accepted Date: 13 October 2015

Please cite this article as: E. Guenther, N. Klein, P. Mikus, M.K. Stehling, B. Rubinsky, Electrical breakdown in tissue electroporation, *Biochemical and Biophysical Research Communications* (2015), doi: 10.1016/j.bbrc.2015.10.072.

This is a PDF file of an unedited manuscript that has been accepted for publication. As a service to our customers we are providing this early version of the manuscript. The manuscript will undergo copyediting, typesetting, and review of the resulting proof before it is published in its final form. Please note that during the production process errors may be discovered which could affect the content, and all legal disclaimers that apply to the journal pertain.

ACCEPTED MANUSCRIPT

Electrical breakdown in tissue electroporation

Enric Guenther[1,2,3], Nina Klein[1,2,3,*], Paul Mikus[1], Michael K. Stehling[1,3], Boris Rubinsky[1,4]

1 – Inter Science, Reusblickstr 23, 6038 Gisikon, Luzern, Switzerland
2 – The first two authors have contributed equally to this paper
3 – Institut fuer Bildgebende Diagnostik, Strahlenbergerstrasse 110, 63067 Offenbach, Germany
4 – Department of Mechanical Engineering, University of California Berkeley, Berkeley, CA 94720, USA

* To whom the correspondence should be addressed at

ACCEPTED MANUSCRIPT

Abstract

Electroporation, the permeabilization of the cell membrane by brief, high electric fields, has become an important technology in medicine for diverse application ranging from gene transfection to tissue ablation. There is ample anecdotal evidence that the clinical application of electroporation is often associated with loud sounds and extremely high currents that exceed the devices design limit after which the devices cease to function. The goal of this paper is to elucidate and quantify the biophysical and biochemical basis for this phenomenon. Using an experimental design that includes clinical data, a tissue phantom, sound, optical, ultrasound and MRI measurements, we show that the phenomenon is caused by electrical breakdown across ionized electrolysis produced gases near the electrodes. The breakdown occurs primarily near the cathode. Electrical breakdown during electroporation is a biophysical phenomenon of substantial importance to the outcome of clinical applications. It was ignored, until now.

Keywords

irreversible electroporation; electrolytic electroporation; tissue ablation; magnetic resonance imaging; electrolysis; NanoKnife

Introduction

Electroporation, the permeabilization of the cell membrane through the application of brief, high strength electric fields across cells has many important medical and biotechnological applications [1,2]. The permeabilization can be reversible or irreversible, as a function of electric field parameters such as strength, duration and shape [3]. The strength of the electric fields in irreversible electroporation is several factors higher than in reversible electroporation, and the treatment entails the application of up to hundreds of microsecond and nanosecond electric pulses [4]. Reversible electroporation is used for insertion of drugs, genes and large molecules into the permeabilized cells, both *in vitro* and *in vivo*. The various applications of reversible electroporation include vaccination, DNA and CRISPR insertion and treatment of cancer with cytotoxic drugs [5-9]. Non-thermal irreversible electroporation (NTIRE) is a molecularly selective, minimally invasive tissue ablation technology used for treatment of cancer and other tissue ablation applications [10,11]. NTIRE selectively affects the cell membrane and spares the extracellular matrix. Although very recent, NTIRE has become an important surgical modality for treatment of non-resectable pancreatic and hepatic tumors, due to its molecular selectivity [12-15].

Typical NTIRE treatment protocols employ electrode needles inserted in parallel with each other, at the boundaries of the undesirable tissue (tumor). Electroporation is generated by delivering high strength electric fields between the electrodes. This study will try to elucidate a physical phenomena that is observed often in clinical use of NTIRE and, occasionally, in clinical use of reversible electroporation, in which the application of electroporation is accompanied by loud sounds and occasional breakdown of the electrical circuit due to currents above the design limit of the electroporation devices.

The goal of this paper is to illuminate the biophysical and biochemical basis for these phenomena. Our hypothesis is that they are caused by electric breakdown across ionized electrolysis produced gases near the electrodes. The hypothesis is based on a number of recent studies, which demonstrate that electrolysis occurs near the electrodes during electroporation [16-21], especially in NTIRE where the current and the delivered charge are high and never accounted for [20]. To eliminate any harm to patients during this study we have developed a new experimental technique that combines clinical data with the use of a tissue phantom and measurements made with medical ultrasound, a microphone, MRI and optical recording.

Materials and Methods

The gathered clinical data was subject to USA Federal Exemption Category four and Category five. It was obtained from standard, routine clinical treatment of prostate cancer with NTIRE. No change was made in the treatment protocol for the purpose of this study. The data used in the study was separated from the identity of the patients to make identification of the patients impossible. The clinical treatment was delivered using a NanoKnife® NTIRE system (Angiodynamics, Latham, NY, USA) and employed commercial NanoKnife® electrodes (Gauge 16, 20 cm). In typical fashion to all clinical procedures of NTIRE, the electrodes are inserted in tissue under ultrasound monitoring and the treatment is continuously monitored with ultrasound (BK Medical Flex Focus, 8848 endorectal biplane transducer, Analogic Ultrasound, Analogic Corporation, 8 Centennial Drive, Peabody, MA, USA). The results shown in this paper are from typical NTIRE treatment protocols in which ninety, 90 microsecond long pulses were delivered between two needle electrodes at a frequency of 1 Hz. The needle electrodes had an active length of 1.5 cm and were inserted in parallel, separated by 1.5 cm. The NanoKnife® power supply is designed to deliver the pulses from a discharging capacitor in groups of ten, after which the capacitor is recharged for the next group of ten pulses. The device records and displays the voltages delivered and the current through the system during the delivery of the pulses. The only change made in a typical procedure, for the purpose of this study, was to place a microphone to quantitatively record the intensity of the sounds emanating from the treatment site. The peak sounds pressure in dB was measured with a microphone (Auna MIC-900B USB condensator microfon, Chal-Tec GmbH, Wallstrasse 16, 10179 Berlin, Germany) placed at a fixed distance of approximately 25 cm from the electroporation treatment site, in a way that it did not interact with the patient and did not interfere with the procedure. The data was analyzed by correlation of: voltage, current, ultrasound and sound during the procedure.

To elucidate the biochemical and biophysical phenomena associated with the sounds obtained, we have used a tissue phantom model, which we have employed in the past for a number of fundamental studies on electroporation. This phantom was used to show that typical electroporation protocols also simultaneously produce electrolytic reactions at the electrodes [20] and that the extent of electrolysis can be monitored in real time with magnetic resonance imaging [16], as well as with electrical impedance tomography [17]. The tissue phantom model is a physiological saline based agar gel. Here, 1% w/v agar (Bacto-Agar, Fischer Scientific International Inc., Hampton, New Hampshire) in 0.9% w/V physiological NaCl solution was brought to boiling, poured into jars of 10 x 10

x 10 cm and cooled at room temperature. The same Angiodynamics NanoKnife® system used in clinical procedures was used to deliver the electroporation pulses in the gel phantom. Two insulated monopolar probes (Gauge 16, 20 cm long) were placed in the gel in parallel with each other, in a plane normal to the outer surface of the gel at approximately 6 cm depth at a distance of 1.5 cm to one another and an exposure length of 1 cm. They were stabilized in place with a default 5 mm Brachy grid. The electroporation protocol was an exact repeat of the clinical protocol. Essentially, 90 pulses were delivered between the electroporation protocol at a frequency of 1 Hz and in groups of ten. The voltage and currents were recorded from the NanoKnife® console output, in an identical way to that in the clinical study. The process of electroporation was recorded with the same ultrasound system used in the clinical procedures. The sound pressure was measured with the identical microphone placed at a fixed distance of 50 cm from the electroporation assembly. A camera (Sony A7, 1-7-1 Konan, Minato-ku, Tokyo 108-0075, Japan) was positioned vertically to the plane of the electrodes to visually record the events near the electrodes using 60 fps full-HD recording with 1/60 s shutter time. In repeat experiments, the gel samples were removed from the experiment site after a predetermine number of pulses and inserted into an MRI (1.5 T Avanto, Siemens, Erlangen) approximately 90 seconds after the last pulse to evaluate the extent of electrolysis after these number of pulses with T2 turbo spin echo sequences in 8 channel head-coil, TR=2400, TE=100.

Our experimental strategy was to examine the hypothesis, without any interference with the optimal treatment procedure for the benefit of the patient. To this end, for each clinical procedure, we repeated the clinical protocol in the gel phantom. We recorded the voltage, current, ultrasound image and sound pressure in both clinical and gel phantom electroporation protocols. This was done to verify that the gel phantom produces similar data as the clinical data, with respect to parameters that can be measured in a patient. Then, we added two measurements to the gel phantom experiments that cannot be done in a patient: MRI examination to demonstrate that the phenomena is associated with products of electrolysis, and optical recording of the experiments near the electrodes to examine our hypothesis that an electric discharge occurs.

Results and Discussion

As mentioned in the materials and methods section, our research strategy is to examine similar treatment protocols in clinical applications and in gel phantoms. We have analyzed five cases. The results were consistent among all the experiments. For illustration purpose, we show experimental data from one of those experiments. Figure 1 illustrates measurements from a clinical NTIRE treatment of the prostate in which two electrode needles, with an exposed active length of 1.5 cm, were inserted in parallel to each other in a prostate cancer tumor. The separation between the electrodes is a standard 1.5 cm. The treatment entailed the delivery of 90, one hundred microsecond long electroporation pulses and delivery voltage dial was set to 2200 V, being standard clinical NTIRE parameters.

Panel A displays the delivered voltage as a function of the pulse number. The data points here, as well as in all the other panels, represent the actually measured data

during each pulse. The connections between the data points have no meaning, except for better visualization of the data. Consistent with the design of the device, the voltage delivered is obtained from the discharge of a capacitor. The electric pulses are delivered in decades of pulses, after which the capacitor is recharged. This is done to maintain the delivered voltage in a relatively narrow range. In panel A, the range is approximately 2200-2000 V, i.e. a variation of 10%, and the pattern of voltage decay in one decade is the same in all the decades.

Panel B displays the current as a function of the electroporation pulse number. A constant impedance between electrodes would result in a current pattern that follows the pattern of the voltage and varies within a decade of pulses by about 10%. Some studies report that tissue can change its impedance with electroporation pulses [22]. However, these changes are monotonic and would not cause major changes in currents within a decade of pulses. The pattern of currents shown in figure 1 panel B is unexpected. We find that after the third decade of pulses, the currents begin to fluctuate wildly and for larger number of pulses. The changes in current across the electroporation pulse decades can be as large as 30% (in some of the experiments the change in currents within one decade was as high as 50%). Furthermore, there is a pattern. The highest currents are generated at the start of the decade and the magnitude of the currents usually decreases towards the end of the decade. In some cases the current at the start of the decade exceeds the limit of the device (50 A), and the device shuts down. This can be very detrimental to the clinical treatment and is a key reason why we tried to elucidate the mechanism involved.

Panel C displays the change in sound intensity in dB, from ambient level, as a function of pulse number. It is evident that the sound intensity expressed in a log scale increases substantially after about 50 pulses. Interestingly, this is also when the fluctuations in currents become very large. This result is consistent in all the clinical experiments. It indicates that there is a correlation between the increase in sound level and the increase in current. The change is with about 30 dB substantial.

Lastly, panel D shows endorectal ultrasound images during a typical NTIRE procedure of a prostate gland with a stage T3 prostate cancer. The treatment shown in this figure was carried out with a total of six electrodes, as two needle treatments are rare in the prostate. The first figure from the left shows two of them, marked as bright spots. They were randomly chosen to function as an *in vivo* comparison, with all following measurements and considerations being attached to them. The figure shows that increasing the number of delivered pulses generates a hyperintense feature around the electrodes. The dimensions of that feature increase with the number of pulses, as shown by the tracing around it. We have discussed this phenomenon in the past [20]. It is attributed to the electrolysis produced gas around the electrodes and the ultrasound wave reflections at the interface between the mismatched acoustic impedance of gas and tissue. It should be noted that because the two electrodes are part of a six probe constellation, the total quantity of gas seen in the figure cannot be fully accounted to the shown pair of two electrodes. Nonetheless, the above described effect is legitimate.

Special considerations went into the design of the gel phantom experiment. Our hypothesis is that the sound and the increased current during electroporation are caused

by electrical breakdown across the electrolysis produced gas layer around the electrodes. To visualize the electrical discharge, the tissue model needs to be transparent. Because the hypothetic dominant mechanism is electrolysis, we used physiological saline to produce the gel. Furthermore, to produce equal amounts of electrolytic products as in tissue, we designed the electroporation parameters in such a way that the currents (i.e. the charge delivered) was similar in the gel experiment to the clinical use in tissue. Because the conductivity of a gel is higher than that of tissue, we employed lower electroporation voltages to keep the current (and thus electrolysis amount) similar to the *in vivo* measurement. The significance of this difference between the gel phantom and clinical data results will be discussed at the end of the discussion of figure 2.

Figure 2 shows typical results obtained for the gel phantom. Panel A illustrates the delivered voltage as a function of pulse number. It is seen that the voltage delivery pattern is identical to that in the clinical application. However, the voltages across a decade of pulses in the gel range from 1500-1200 V, rather than from 1950-2200V in tissue. The experiment was designed so that the currents in the gel range from about 28-40 A, similar to the range in tissue.

Comparing the currents in the gel (panel B figure 2) with those in the tissue (panel B figure 1), we observe a similar pattern. The pattern in the gel is more disciplined than in tissue, obviously due to the homogeneity of the gel. However, overall, the tissue current and the gel currents follow the same paradigm. Within each decade of pulses the current is highest for the first pulse of the decade and decreases towards the last pulse of the decade. This pattern is repeated from decade to decade. The range of currents within a decade increases substantially with each higher decade. The overall increase in current range, between the first and last decade, is by an order of magnitude, in both the gel and the tissue.

Panel C of figure 2 shows the sound pressure in dB. It is evident that the sound intensity during the pulses is high, up to about 25 dB above the ambient. The range is comparable to that in the clinical measurement, which had values around 30 dB. For lower decades of pulses, below the fifth decade the sound intensity from the gel fluctuates. However, similarly to tissue (panel C figure 1), after about the fifth decade the sound intensity remains constantly high. The high sound intensity at the later pulse decades corresponds well with the wide excursions in currents in the last pulse decades, for both tissue and gel.

The ultrasound appearance during the delivery of electroporation pulses in the gel is shown in panel D of figure 2. The first photograph on the left shows the ultrasound signature of the electrodes. Similarly to the ultrasound in tissue (panel D figure 1), a hyperintense ultrasound feature forms around the electrodes, which increases with the number of pulses. However, the hypertense region in the gel phantom does not extend as far as in the prostate, which might partly be attributed to the fact that the prostate, as a gland organ, has pathways in which pressure from the discharges causes further spreading than in the compact agar. Additionally, as noted previously, the *in vivo* images were taken during a treatment with a six probe constellation, which would augment the bigger hyperintense region.

Panels A, B, C and D in figures 1 and 2 show that electroporation pulses produce a similar effect in tissue and in the gel phantom. The voltage, current, sound pressure and ultrasound signature exhibit a qualitatively similar dependence on pulse number in the gel and tissue. Therefore, it is reasonable to assume that similar biophysical/biochemical phenomena are responsible for the observed behavior in media.

Panels E, F and G, in figure 2 were obtained from measurements that cannot be done during clinical treatment of patients. Panels E and F display the T2 weighted MRI of the treated gel after different numbers of pulses. Panel E is for a cross section normal to the plane of the electrodes and panel F is for a cross section in a plane along the electrodes. The left electrode is the anode, the right one the cathode. We have shown from basic biophysical principles that the change in T2 weighted MRI intensity signature around the electrodes corresponds to a change in pH, and is a consequence of the process of electrolysis [16]. Specifically, in a physiological saline solution, H_2 forms at the anode and Cl_2 forms at the cathode. It is evident that the extent of the affected region increases with the number of pulses. The right hand side photograph in panels E and F show that near the cathode, after 90 pulses, the gel is warped. Both panels demonstrate that a process of electrolysis has occurred near the electrodes in our specific electroporation experiments.

Panel G in figure 2 is the central result of this study. It shows a photograph of the electrodes through the gel for various pulse numbers. An electric discharge is seen at the cathode as bright areas. After ten pulses, the electrical discharge is seen at the tip of the electrodes, while after 40 pulses it occurs at the tip and at the upper edge of the exposed part of the electrode. And finally, after 90 pulses, a violent discharge surrounds the electrodes completely. The observed pattern is typical for electrical breakdown across ionized gases at atmospheric pressures [23]. With the products of electrolysis being H_2 at the anode and Cl_2 at the cathode, the cathode supplies the electrons for the discharge, which occurs when the electric field exceeds the breakdown voltage. The discharge begins at the edges of the electrode, where the highest electromagnetic field occurs. In this study, the gases that form around the electrodes insulate the electrodes from the surrounding tissue. Therefore, the pulsed voltage induced electric field develops across the gas layer. When the electric field across the gas layers increases above the breakdown voltage, a violent discharge occurs accompanied with light from the ionized gases and a sudden increase in the current between the electrodes. This discharge also produces the violent sound. Taken together, all the panels in figure 2 suggest that this is the mechanism responsible for the loud sounds heard during clinical electroporation and the sudden increase in current. Panel F also shows that the volume of the electric discharge increases with number of pulses. This is consistent with the increase in extent of electrolysis with the number of pulses. The very high currents that occur during the first high voltage pulse in the decade of pulses can be also explained through this mechanism. At the end of the decade, the voltage is lower and is not sufficient to produce the breakdown. It is possible at an equilibrium point. The sudden increase in voltage at the start of the new decade of pulses causes the violent breakdown to occur, after which the system returns to a new equilibrium – which is disrupted when a new decade of pulses begins.

The only difference between the experimental parameters in tissue and in the gel is the applied voltage. The voltage in the gel is lower to produce a similar amount of electrolytic products in a higher conductivity medium. However, the breakdown point for the electrical discharge is a function of the critical electric field. This is the voltage difference across the electrolysis produced gas layer, divided by the thickness of the gas layer. It is reasonable to state that if an electric discharge is observed in a gel in which the electroporation pulses are delivered at a lower voltage, the same phenomenon will occur in tissue. Considering the absolute sound pressure, we can say that it is significantly louder *in vivo* than in the phantom, even though the electrodes *in vivo* were shielded by about 20 cm of tissue, while it was approximately 5 cm in the gel. This could lead to the assumption that the phenomenon was more pronounced *in vivo* than in gel, which would also coincide with the higher voltage measured.

In conclusion, this study has produced circumstantial evidence that clinical electroporation protocols produce electrical breakdown across electrolytically produced layers of gases around the electrodes. We suggest that these are the sources of loud sounds and sudden increases in current during clinical electroporation. The phenomenon is particularly pronounced in electroporation with large numbers of pulses, typical to NTIRE. The electrical breakdown and the associated pressure waves can cause substantial damage to tissue; in particular in regions surrounded by a rigid tissue structure, such as the brain or the prostate. These pulses also affect the controlled delivery of electroporation. The electric breakdown in tissue was not studied before. However, it may have important consequences on clinical protocols. One area of possible research may be to devise electroporation protocols that minimize or eliminate the electric breakdown. This study shows that these electric breakdowns and surges in currents are associated with the mode in which the pulses are delivered; in the form of decades of pulses with high voltages at the start of each decade. The observed phenomenon may be eliminated by delivering the pulses in different ways. A possibility could be to deliver the pulses as continuously decreasing voltages to avoid the generation of a critical breakdown electric field when the electrodes are surrounded by the electrolytically produced gases. Another way could be changing the polarity of the electrodes after each pulse or delivering the pulses at a lower frequency to facilitate the diffusion of the gases. In summary, now that this previously ignored biochemical/biophysical phenomenon has been identified, it must be further investigated.

References

[1] E. Neumann, M. Schaeffer-Ridder, Y. Wang, P.H. Hofschneider, Gene transfer into mouse lymphoma cells by electroporation in high electric fields, EMBO J, 1 (1982) 841-845.
[2] S. Haberl, D. Miklavcic, G. Sersa, W. Frey, B. Rubinsky, Cell Membrane Electroporation-Part 2: The Applications, Ieee Electrical Insulation Magazine, 29 (2013) 29-37.
[3] J.C. Weaver, Y.A. Chizmadzhev, Theory of electroporation: a review, Bioelectrochem. Bioenerg., 41 (1996) 135-160.

[4] J.C. Weaver, K.C. Smith, A.T. Esser, R.S. Son, T.R. Gowrishankar, A brief overview of electroporation pulse strength-duration space: A region where additional intracellular effects are expected, Bioelectrochemistry, 87 (2012) 236-243.
[5] M.J. Jaroszeski, R. Gilbert, C. Nicolau, R. Heller, In vivo gene delivery by electroporation, Advanced applications of electrochemistry, 35 (1999) 131-137.
[6] L.M. Mir, S. Orlowski, J.J. Belehradek, C. Paoletti, Electrochemotherapy potentiation of antitumour effect of bleomycin by local electric pulses European Journal of Cancer, 27 (1991) 68-72.
[7] S.A. Shirley, R. Heller, L.C. Heller, Electroporation Gene Therapy, 2014.
[8] M. Hashimoto, T. Takemoto, Electroporation enables the efficient mRNA delivery into the mouse zygotes and facilitates CRISPR/Cas9-based genome editing (vol 5, 11315, 2015), Scientific Reports, 5 (2015).
[9] M. Hashimoto, T. Takemoto, Electroporation enables the efficient mRNA delivery into the mouse zygotes and facilitates CRISPR/Cas9-based genome editing, Scientific Reports, 5 (2015).
[10] B. Rubinsky, G. Onik, P. Mikus, Irreversible electroporation: A new ablation modality - Clinical implications, Technology in Cancer Research & Treatment, 6 (2007) 37-48.
[11] M. Phillips, E. Maor, B. Rubinsky, Nonthermal Irreversible Electroporation for Tissue Decellularization, Journal of Biomechanical Engineering-Transactions of the Asme, 132 (2010).
[12] K. Thomson, S.T. Kee, Clinical Research on Irreversible Electroporation of the Liver, Clinical Aspects of Electroporation, (2011) 237-246.
[13] W. Cheung, H. Kavnoudias, S. Roberts, B. Szkandera, W. Kemp, K.R. Thomson, Irreversible Electroporation for Unresectable Hepatocellular Carcinoma: Initial Experience and Review of Safety and Outcomes, Technology in Cancer Research & Treatment, 12 (2013) 233-241.
[14] K.R. Thomson, H. Kavnoudias, R.E. Neal, 2nd, Introduction to Irreversible Electroporation-Principles and Techniques, Techniques in vascular and interventional radiology, 18 (2015) 128-134.
[15] R.C.G. Martin, 2nd, D. Kwon, S. Chalikonda, M. Sellers, E. Kotz, C. Scoggins, K.M. McMasters, K. Watkins, Treatment of 200 Locally Advanced (Stage III) Pancreatic Adenocarcinoma Patients With Irreversible Electroporation: Safety and Efficacy, Annals of surgery, 262 (2015) 486-494.
[16] A. Meir, M. Hjouj, L. Rubinsky, B. Rubinsky, Magnetic Resonance Imaging of Electrolysis, Scientific Reports, 5 (2015).
[17] A. Meir, B. Rubinsky, Electrical impedance tomography of electrolysis, PloS ONE, 10 (2015) e0126332-e0126332.
[18] M. Phillips, N. Raju, L. Rubinsky, B. Rubinsky, Modulating electrolytic tissue ablation with reversible electroporation pulses., Technology, 3 (2015) 1-19.
[19] M. Phillips, L. Rubinsky, A. Meir, N. Raju, B. Rubinsky, Combining Electrolysis and Electroporation for Tissue Ablation, Technology in cancer research & treatment, 14 (2015) 395-410.
[20] L. Rubinsky, E. Guenther, P. Mikus, M. Stehling, K.,, B. Rubinsky, Electrolytic Effect During Tissue Ablation by Electroporation., Technology in cancer Research and Treatement., (2015).

[21] G.D. Troszak, B. Rubinsky, Self-powered electroporation using a singularity-induced nano-electroporation configuration, Biochemical and Biophysical Research Communications, 414 (2011) 419-424.
[22] A. Ivorra, B. Rubinsky, In vivo electrical impedance measurements during and after electroporation of rat liver, Bioelectrochemistry, 70 (2007) 287-295.
[23] J.D. Cobine, Gaseous Conductors: Theory and Engineering Applications, Dover, New York, 1958.

Fig.1: *In vivo* data of a NTIRE treatment of the prostate.
The parameters were: Electrode spacing 1.5 cm, set voltage 2200 V, and 90 pulses with 90 microsecond length. Voltage (A) and current (B) were logged by the NanoKnife system. Sound intensity was measured in a constant distance using a capacitor microphone and calculated relatively to the mean ambient noise (C). (D) shows the gas production *in vivo* in an ultrasound image after 10 (left), 40 (middle) and 90 (right) pulses. Sound intensity rises significantly and gas clouds a major area in the ultrasound image.

Fig.2: Measurements in an agar gel phantom.
The voltage and current is shown in (A) and (B), respectively. The sound intensity above mean ambient noise of every pulse is shown in (C). (D), (E), (F) and (G) show ultrasound, transversal T2 MRI, longitudinal T2 MRI and visual capture respectively after 10 (left), 40 (middle) and 90 pulses (right). MRI (E + F) show significant pH changes around both electrodes (anode left, cathode right). The visual (G) and the ultrasound (D) illustrate that discharges happen mainly at the cathode with increasing intensity.

ACCEPTED MANUSCRIPT

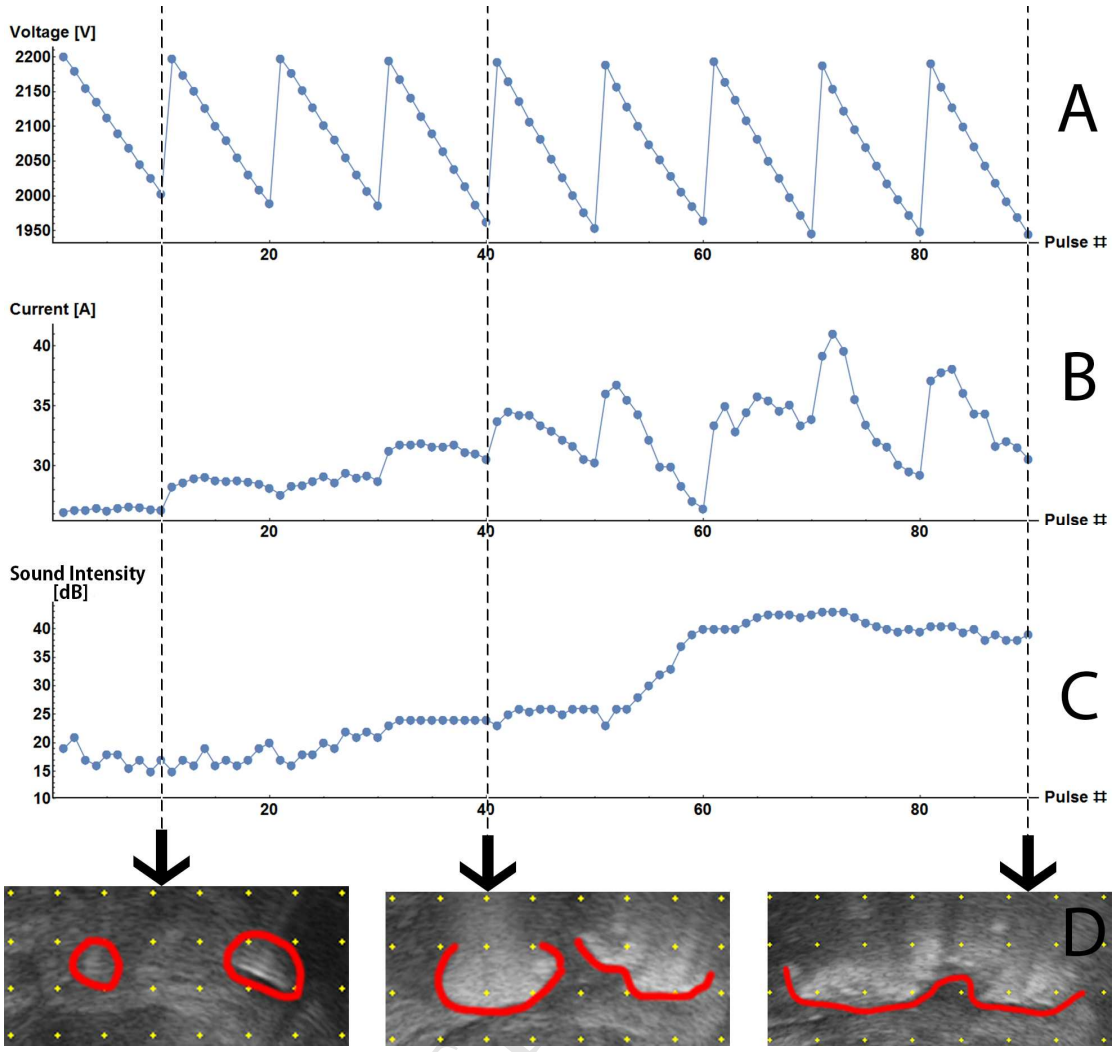

ACCEPTED MANUSCRIPT

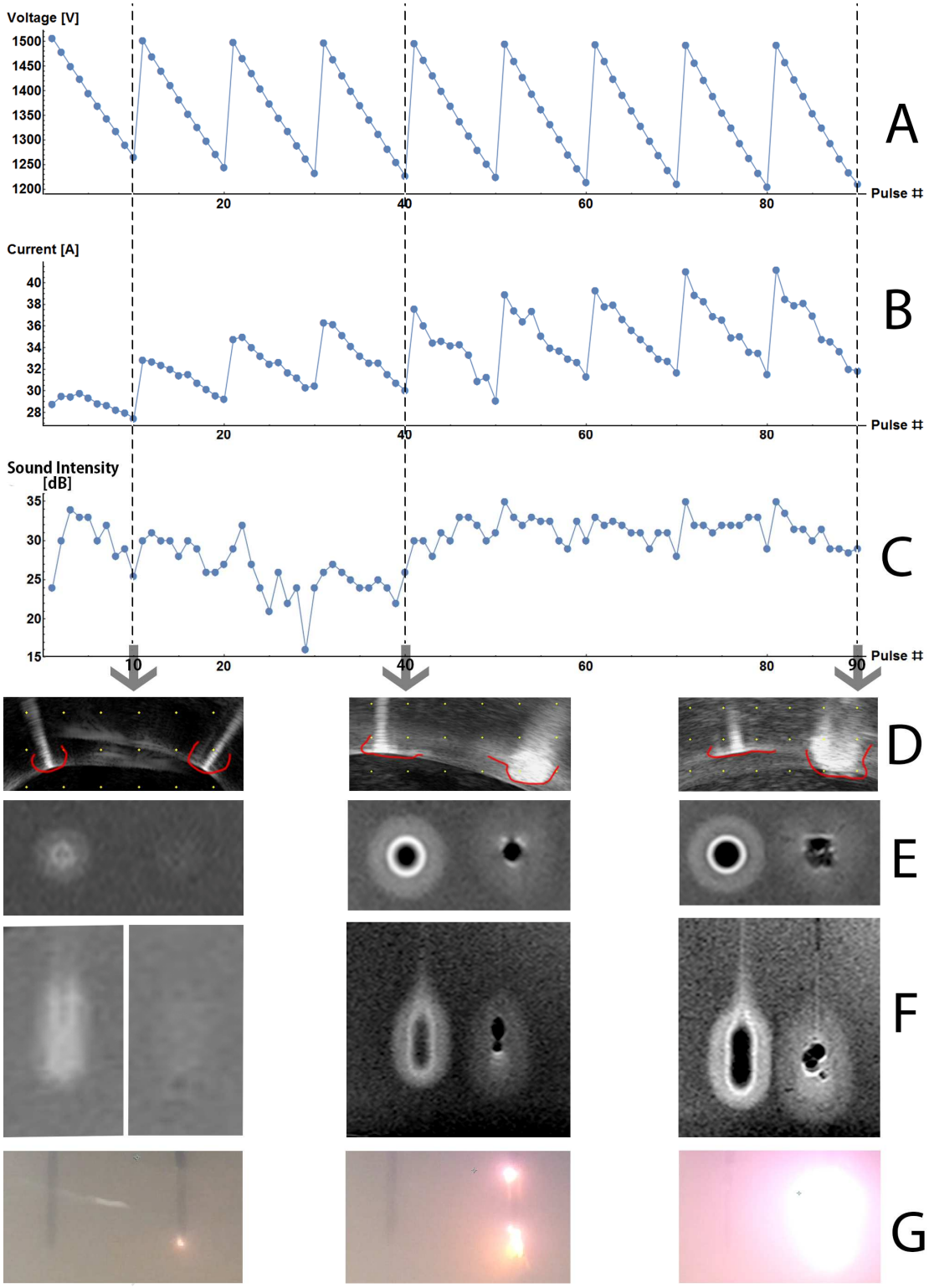
Voltage [V]
1500
1450
1400
1350
1300
1250
1200
20
40
60
80
Pulse #
A
Current [A]
40
38
36
34
32
30
28
20
40
60
80
Pulse #
B
Sound Intensity [dB]
35
30
25
20
15
10
20
40
60
80
90
Pulse #
C
D
E
F
G

ACCEPTED MANUSCRIPT

Highlights

- In clinical application, electroporation is often associated with high currents, visible gas production in ultrasound and loud sounds.
- We deliver evidence that the phenomenon is caused by electrical breakdown across ionized electrolysis produced gases near the electrodes.
- These electric breakdowns are associated with the total amount of electrolysis produced, the voltage but also the mode and protocols in which the pulses are delivered. All should be respected when finding optimal treatment protocols.

ACCEPTED MANUSCRIPT